The Plant Cell, Vol. 17, 1141–1153, April 2005, www.plantcell.org

The Critical Role of Disulfide Bond Formation in Protein Sorting in the Endosperm of Rice

Yasushi Kawagoe,[a,1] Kazuya Suzuki,[a,b] Mikako Tasaki,[c] Hiroshi Yasuda,[a] Kayo Akagi,[d] Etsuko Katoh,[d] Naoko K. Nishizawa,[b] Masahiro Ogawa,[c] and Fumio Takaiwa[a]

[a] Department of Plant Biotechnology, National Institute of Agrobiological Sciences, Tsukuba, Japan 305-8602
[b] Laboratory of Plant Biotechnology, University of Tokyo, Bunkyo-ku, Tokyo, Japan 113-8657
[c] Department of Life Science, Yamaguchi Prefectural University, Sakurabatake, Yamaguchi, Japan 753-8502
[d] Department of Biochemistry, National Institute of Agrobiological Sciences, Tsukuba, Japan 305-8602

Many seed storage proteins, including monomeric 2S albumin and polymeric prolamin, contain conserved sequences in three separate regions, termed A, B, and C, which contain the consensus motifs LxxC, CCxQL, and PxxC, respectively. Protein-sorting mechanisms in rice (*Oryza sativa*) endosperm were studied with a green fluorescent protein (GFP) fused to different segments of rice α-globulin, a monomeric, ABC-containing storage protein. The whole ABC region together with GFP was efficiently transported to protein storage vacuoles (type II protein bodies [PB-II]) in the endosperm cells and sequestered in the matrix that surrounds the crystalloids. Peptide Gln-23 to Ser-43 in the A region was sufficient to guide GFP to PB-II. However, GFP fused with the AB or B region accumulated in prolamin protein bodies. Substitution mutations in the CCxQL motif in the B region significantly altered protein localization in the endosperm cells. Furthermore, protein extracts containing these substituted proteins had increased amounts of the endoplasmic reticulum (ER) chaperons BiP (for binding protein), protein disulfide isomerase, and calnexin as a part of protein complexes that were insoluble in a detergent buffer. These results suggest that the ER chaperons and disulfide bonds formed at the dicysteine residues in CCxQL play critical roles in sorting fused proteins in the endosperm cells.

INTRODUCTION

Seed storage proteins are often classified based on their solubilities in different solvents (Shewry and Casey, 1999). As an example, the major seed storage proteins in rice (*Oryza sativa*) are acid- or alkaline-soluble glutelins (11S globulin homologs), saline-soluble α-globulin, and alcohol-soluble prolamins (Bechtel and Juliano, 1980; Oparka and Harris, 1982; Krishnan et al., 1986; Yamagata and Tanaka, 1986). Although this classification is convenient in terms of protein handling, it does not necessarily reflect the evolutionary relationships between storage proteins. For example, Kreis et al. (1985) reported that prolamins, a major class of seed storage proteins in cereals (Shewry and Tatham, 1999), and water-soluble 2S albumins in dicotyledonous plants contain homologous sequences in three separate regions, termed A, B, and C. The three-dimensional structures of 2S albumins in sunflower (*Helianthus annuus*; SFA-8) (Pandya et al., 2000; Pantoja-Uceda et al., 2004) and castor bean (*Ricinus communis*; RicC3) (Pantoja-Uceda et al., 2003) revealed that these proteins are part of a superfamily of proteins whose structure is described as ''4 helices; folded leaf; right-handed superhelix; disulfide rich'' (Murzin et al., 1995).

Rice prolamins constitute a large gene family and account for 20 to 25% of all seed proteins (Ogawa et al., 1987; Li and Okita, 1993; Muench et al., 1999). Some rice prolamins contain the characteristic ABC sequences described above; however, unlike monomeric 2S albumins, the ABC-containing prolamins are stored in the form of polymers or aggregates in spherical intracisternal inclusion granules, referred to as type I protein bodies (PB-I), within the endoplasmic reticulum (ER) lumen (Mitsukawa et al., 1999; Muench et al., 1999). Recent studies have reported that the mRNAs of these prolamins associate with protein body ER, whereas the mRNAs of glutelins associate with cisternal ER (Crofts et al., 2004).

Rice α-globulin, encoded by a single gene (Shorrosh et al., 1992), contains the ABC regions of storage proteins and constitutes up to 12% of all of the seed proteins produced (Krishnan and White, 1995). This protein is 49% α-helix, based on the circular dichroism spectrum of the purified protein (Pan and Reeck, 1988). An immunocytochemical study reported that α-globulin accumulates in Golgi-associated vesicles (Krishnan et al., 1992), which presumably transport α-globulin to the protein storage vacuoles, which hereafter are referred to as type II protein bodies (PB-II). PB-II also store glutelins as crystalloids (crystal-like blocks in which lattice structures are often formed). In PB-II, α-globulin is sequestered in the matrix that surrounds these crystalloids (Bechtel and Juliano, 1980; Krishnan et al., 1992).

[1] To whom correspondence should be addressed. E-mail kawagoe@nias.affrc.go.jp; fax 81-29-838-8397.
The author responsible for the distribution of materials integral to the findings presented in this article in accordance with the policy described in the Instructions for Authors (www.plantcell.org) is: Yasushi Kawagoe (kawagoe@nias.affrc.go.jp).
Article, publication date, and citation information can be found at www.plantcell.org/cgi/doi/10.1105/tpc.105.030668.

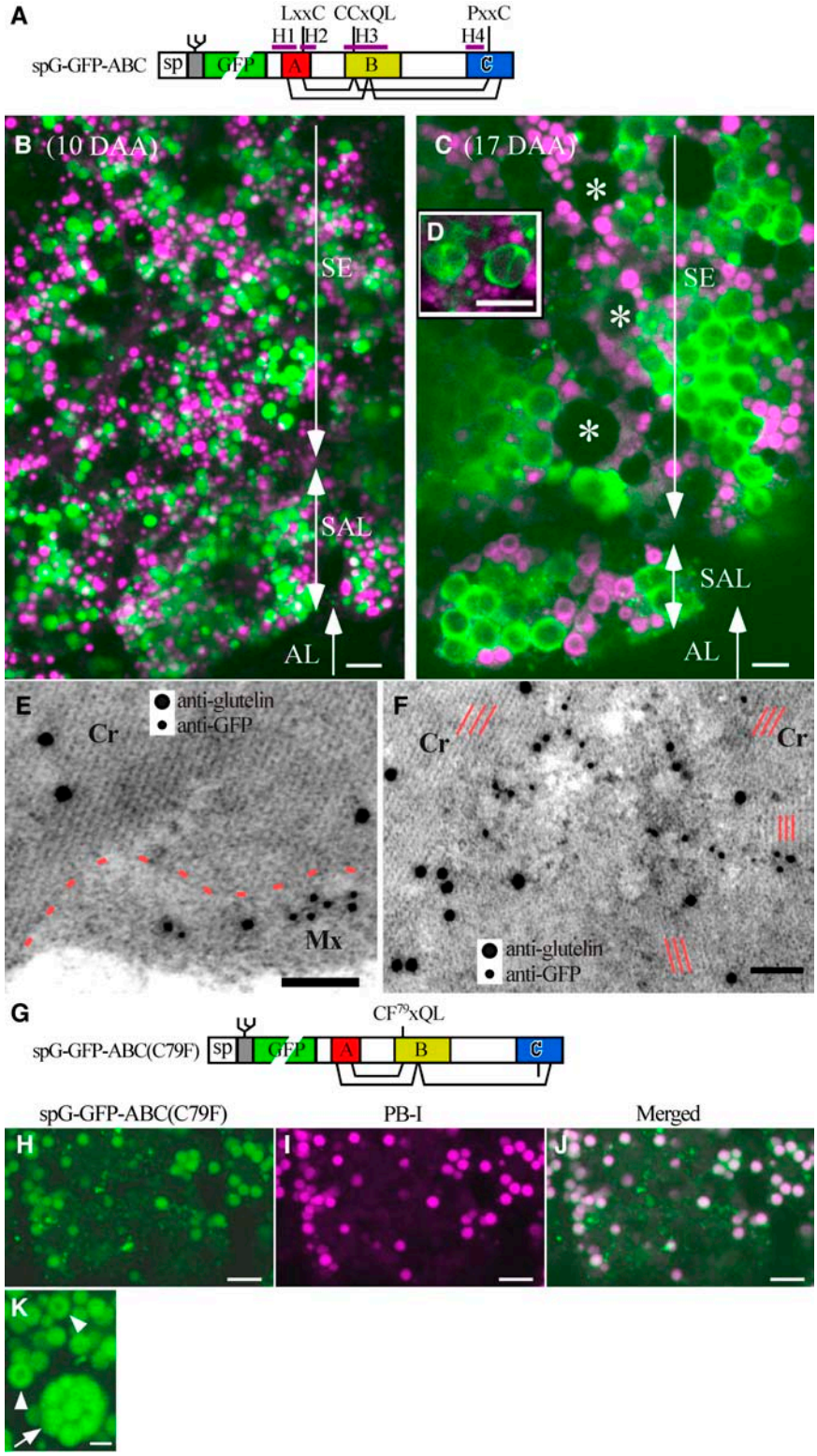

Figure 1. The Single Amino Acid Substitution at Cys-79 of α-Globulin Dramatically Alters Protein Localization.

(A) Scheme of GFP fused to α-globulin. A synthetic peptide (gray bar) containing an *N*-glycosylation site is inserted between a signal peptide (sp) and GFP (green). The PHD program (Rost and Sander, 1993) predicted the four α-helices H1 (Glu-26 to Val-40), H2 (Leu-45 to Gln-55), H3 (Leu-74 to

Chaperon proteins in the ER lumen are crucial for the biogenesis of PB-I. The binding protein (BiP) forms complexes with nascent prolamin polypeptides (Li et al., 1993; Muench et al., 1997). Recent characterizations of the *endosperm storage protein2* (*esp2*) mutant demonstrated that another chaperon protein, protein disulfide isomerase (PDI), is required for the segregation of prolamins and proglutelins in the ER lumen (Takemoto et al., 2002), which suggests that PDI assists disulfide-interchange reactions involving prolamins and proglutelins. However, little is known about which sequences in prolamins or proglutelins promote interactions with PDI. A third chaperon protein in the ER lumen, calnexin, is involved in the quality control of glycoproteins through interactions with *N*-glycans (Vitale, 2001). However, the role of calnexin in the developing endosperm is poorly understood. The temporary presence of an abundance of unfolded proteins in the ER lumen upregulates many genes, including the ER chaperons (Martinez and Chrispeels, 2003).

In this study, a green fluorescent protein (GFP) is shown to be a valuable molecular probe in studying protein-sorting mechanisms in the rice endosperm. The consensus motifs LxxC, CCxQL, and PxxC were identified in both monomeric and polymeric ABC-containing proteins, and the dicysteine residues in the CCxQL motif of α-globulin were found to play a critical role in protein sorting in the developing endosperm.

RESULTS

An Intramolecular Disulfide Bond in α-Globulin Is Necessary for Protein Transport to the PB-II Matrix

The sequence of rice α-globulin was compared with those of other ABC-containing proteins, including maize (*Zea mays*) α-globulin (Woo et al., 2001), wheat (*Triticum aestivum*) high molecular weight (HMW) glutenins (1By9, 1Dy10, and 1Dy12) (Halford et al., 1987), and sunflower 2S albumin SFA-8 (Pandya et al., 2000; Pantoja-Uceda et al., 2004). LxxC, CCxQL, and PxxC were identified as the most conserved motifs in the A, B, and C regions, respectively (data not shown). The three-dimensional structures of the 2S albumins SFA-8 (Pantoja-Uceda et al., 2004) and RicC3 (Pantoja-Uceda et al., 2003) indicate that all four Cys residues in the three motifs are involved in intramolecular disulfide bonds (Figure 1A). Accordingly, it was predicted that substituting Cys-79 (the second Cys in CCxQL) would eliminate the disulfide bond between Cys-79 and Cys-171 (in PxxC) and that such a drastic alteration in the protein structure might affect the level or localization of the protein in the endosperm cells. Two GFP fusion proteins were constructed: spG-GFP, which contained a signal peptide and an *N*-glycosylation site at the N terminus, was fused to either a wild-type α-globulin (Gly-21 to Tyr-186), producing spG-GFP-ABC (Figure 1A), or an altered protein with Phe substituted at Cys-79, producing spG-GFP-ABC(C79F) (Figure 1G). The fusion genes were expressed under the control of the α-*globulin* promoter in transgenic rice. The GFP fluorescence of spG-GFP-ABC was monitored after staining seed sections with rhodamine B, which preferentially binds prolamins in PB-I (Choi et al., 2000). The protein was primarily found in spherical organelles of ~1 to 3 μm at 10 d after anthesis (DAA) (Figure 1B). However, in the middle stage of seed development (12 to 18 DAA), the protein was detected on the periphery of oval compartments of 3 to 6 μm (Figure 1C). In addition, the proteins often extended into the interior of the structures (Figure 1D). These results indicate that the fusion proteins transported to PB-II were sequestered in the matrix that surrounds crystalloids by 17 DAA. The distribution of spGFP-ABC, which lacks the *N*-glycosylation site, was similar to that of the glycosylated spG-GFP-ABC (data not shown). Immunocytochemical analyses showed that anti-glutelin antibody recognized

Figure 1. (continued).

Glu-103), and H4 (Val-155 to Gln-166). Predicted intramolecular disulfide bonds (Cys-36 to Cys-89, Cys-48 to Cys-78, Cys-79 to Cys-171, and Cys-91 to Cys-178) are indicated with lines. Regions A (red; Asp-33 to Val-51), B (yellow; Arg-75 to Gln-111), and C (blue; Arg-156 to Phe-181) contain LxxC, CCxQL, and PxxC, respectively.

(B) and **(C)** Distinct localizations of spG-GFP-ABC in the endosperm cells at 10 DAA **(B)** and 17 DAA **(C)**. Seed sections were stained with rhodamine B (red fluorescent image was converted to magenta), which specifically binds prolamins in PB-I. Note that at 17 DAA, the fusion protein is present mainly in the matrix of PB-II that surrounds the crystalloids. AL, aleurone cells; SAL, subaleurone cells; SE, starchy endosperm cells. Asterisks indicate amyloplasts. Bars = 5 μm.

(D) High-magnification view of PB-II containing spG-GFP-ABC. Note that the fusion proteins are also present in the gaps between blocks of crystalloids. Bar = 5 μm.

(E) and **(F)** Double immunolabeling of glutelin (10-nm gold particle) and GFP (5-nm gold particle) in PB-II containing spGFP-ABC.

(E) spGFP-ABC is present in the matrix of PB-II. The boundary between the crystalloid and the matrix is marked with a dotted line. Note that the crystalloid has a clear lattice structure. Cr, crystalloid; Mx, matrix. Bar = 50 nm.

(F) spGFP-ABC is detected in the gaps between blocks of crystalloids. Note that the crystalloids contain lattices of different angles (indicated with red parallel lines), suggesting that these crystalloids developed independently in the protein body. Bar = 50 nm.

(G) Scheme of spG-GFP-ABC(C79F). The substitution mutation at Cys-79 in CCxQL with Phe is expected to abolish the intramolecular disulfide bond between Cys-79 and Cys-171 in PxxC.

(H) to **(J)** Distribution of spG-GFP-ABC(C79F) **(H)** and PB-I **(I)** in a subaleurone cell at 16 DAA. The two images are merged in **(J)**. Note that the fusion protein is mainly present in PB-I and is also detectable in the network of cisternal ER. Bars = 5 μm.

(K) High-magnification view of PB-I containing spG-GFP-ABC(C79F) in a starchy endosperm cell at 12 DAA. A projection image of seven GFP fluorescence images taken at 1-μm intervals along the *z* axis. Note that multiple PB-I are present in the dilated ER (arrow). The fusion protein is more concentrated in the periphery of PB-I (arrowheads). Bar = 2 μm.

glutelins in crystalloids with characteristic lattice structures and that anti-GFP antibody recognized the fusion proteins in the matrix of PB-II (Figure 1E). Consistent with the confocal image shown in Figure 1D, spGFP-ABC was also detected in the gaps between blocks of crystalloids (Figure 1F).

By contrast, the substituted protein, spG-GFP-ABC(C79F) (Figure 1G), was mainly found in rhodamine-stained PB-I and was detectable to a significantly lesser extent in the cisternal ER (Figures 1H to 1J). The protein tended to accumulate on the periphery inside PB-I (Figure 1K, arrowheads). In addition, unusual dilated organelles containing multiple PB-I were frequently observed in the endosperm cells (Figure 1K, arrow). Because PB-I develop in the ER lumen, and because PB-I are not subsequently incorporated into vacuoles (Muench et al., 1999), it would be reasonable to perceive the dilated organelle as a form of ER. These results suggest that the disulfide bond between Cys-79 and Cys-171 is necessary for the fusion protein to exit the ER.

Protein levels of spG-GFP-ABC and spG-GFP-ABC(C79F) were similar to that of endogenous α-globulin (Figures 2A and 2B). α-Globulin migrated at the apparent molecular mass of 22 and 26 kD under nonreducing and reducing conditions, respectively (Figures 2A and 2B), suggesting that disulfide bonds were responsible for the high mobility under nonreducing conditions. Likewise, spG-GFP-ABC migrated at the apparent molecular mass of 55 and 60 kD under nonreducing and reducing conditions, respectively. By contrast, spG-GFP-ABC(C79F) was not extractable under nonreducing conditions (Figure 2B), suggesting that it formed intermolecular disulfide bond(s) with other proteins in PB-I and cisternal ER. Both spG-GFP-ABC and spG-GFP-ABC(C79F) were efficiently glycosylated, and the fusion proteins turned out to be the most abundant glycoproteins in the seeds (Figure 2C). The glycans of the two proteins were sensitive to Endo H digestion, indicating that the glycans were not modified to Endo H–resistant, complex types. The protein levels of BiP (72 kD), PDI (66 kD), and calnexin (68 kD) were not significantly different between the transgenic and control plants (Figure 2D). These results suggest that the protein transport in the endomembrane system was not significantly perturbed in the endosperm cells of the transgenic rice.

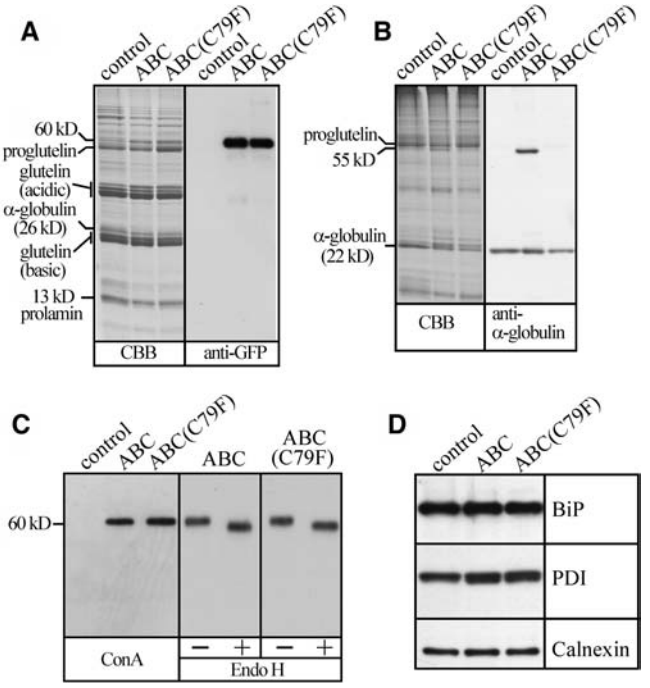

Figure 2. Protein Levels of Glycosylated Fusion Proteins and ER Chaperons.

(A) Left gel: proteins extracted from mature seeds with the urea/SDS buffer under reducing conditions (see procedures in Methods) were separated on a 12% SDS-PAGE gel and stained with Coomassie Brilliant Blue (CBB). Right gel: protein gel blotting with anti-GFP antibody. The fusion proteins and α-globulin migrated at the apparent molecular masses of 60 and 26 kD, respectively. Control lanes, untransformed rice; ABC lanes, spG-GFP-ABC; ABC(C79F) lanes, spG-GFP-ABC(C79F).

(B) Left gel: seed proteins extracted with the urea/SDS buffer under nonreducing conditions were separated on a 12% SDS-PAGE gel and stained with Coomassie Brilliant Blue. Right gel: protein gel blotting with anti-α-globulin antibody. Note that both α-globulin and spG-GFP-ABC were extractable under nonreducing conditions, whereas spG-GFP-ABC(C79F) was not. spG-GFP-ABC and α-globulin migrated at the apparent molecular masses of 55 and 22 kD, respectively.

(C) Left gel: seed proteins were extracted from mature seeds with the urea/SDS buffer under reducing conditions, and peroxidase-conjugated concanavalin A (ConA) was used to detect glycoproteins. Note that the fusion proteins are the most abundant glycoproteins detectable with concanavalin A. Right gel: the proteins were incubated in the presence (+) or absence (−) of Endo H, followed by protein gel blotting with anti-GFP antibody. Note that *N*-glycans are sensitive to Endo H digestion.

(D) Protein gel blot analyses with antibodies against ER chaperons. Seed proteins were extracted with the urea/SDS buffer under reducing conditions. Note that the ER chaperons BiP (72 kD), PDI (66 kD), and calnexin (68 kD) were not upregulated in the seeds of the transgenic plants.

The CCxQL Motif in Region B Plays a Critical Role in Targeting GFP to PB-I

To further characterize the relationship between protein structure and localization in the endosperm cells, the C-terminal sequence (Gly-112 to Tyr-186) was deleted from the PB-II–targeted spGFP-ABC (spGFP-AB, Figure 3A). Interestingly, the truncated protein accumulated in PB-I with high efficiency (Figure 3B). Dilated ERs containing multiple PB-I were frequently observed (Figures 3B to 3D, arrows). The protein often accumulated in the core of PB-I (Figures 3E to 3G, arrowheads). The localization of spGFP-B, which contains all of region B (Arg-68 to Gln-111), was then analyzed (Figure 3H). The distribution of spGFP-B was indistinguishable from that of spGFP-AB (Figures 3I to 3K). Immunostaining analyses with anti-glutelin and anti-GFP antibodies also indicated that spGFP-B was targeted to PB-I (Figures 3L to 3N). An electron microscope immunocytochemical analysis confirmed that spGFP-B was present in PB-I (Figure 3O). The morphology of PB-I was indistinguishable from that in wild-type plants, indicating that

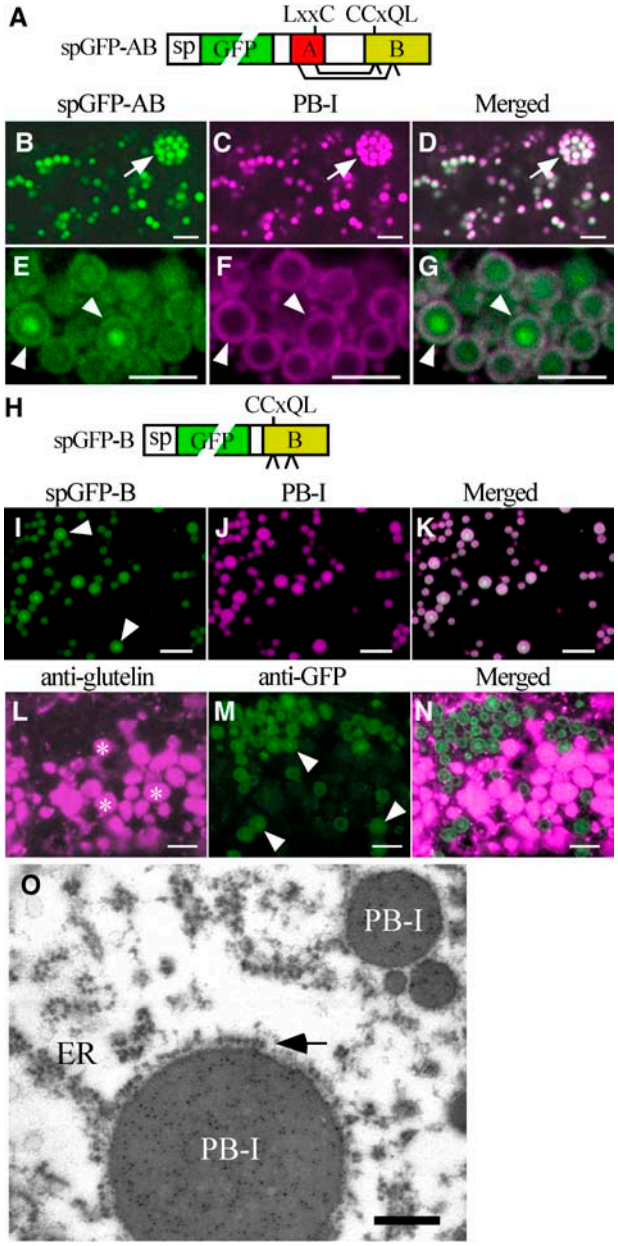

Figure 3. The B Region Efficiently Targets GFP to PB-I.

(A) Scheme of spGFP-AB. Two predicted intramolecular disulfide bonds (Cys-36 to Cys-89 and Cys-48 to Cys-78) are indicated with lines. Free Cys-79 and Cys-91 are indicated with short, unconnected lines.

(B) to **(D)** Distribution of spGFP-AB **(B)** and PB-I **(C)** in a subaleurone cell at 8 DAA. The two images are merged in **(D)**. Note that spGFP-AB was efficiently partitioned into the protein bodies in the dilated ER indicated with the arrows. Bars = 5 μm.

(E) to **(G)** High-magnification views of PB-I. The distribution of spGFP-AB **(E)** and PB-I **(F)** in a subaleurone cell at 18 DAA. The two images are merged in **(G)**. Arrowheads point to PB-I that accumulated spGFP-AB in the core of the protein body. Bars = 5 μm.

(H) Scheme of spGFP-B, which contains four unpaired Cys residues (Cys-78, Cys-79, Cys-89, and Cys-91) indicated with short lines.

(I) to **(K)** The distribution of spGFP-B **(I)** and PB-I **(J)** in a subaleurone cell at 12 DAA. The two images are merged in **(K)**, which shows that spGFP-B accumulated in PB-I.

(L) to **(N)** Immunolabeling of a subaleurone cell with anti-glutelin antibody **(L)** and anti-GFP antibody **(M)**. The two images are merged in **(N)**. Arrowheads in **(M)** point to PB-I that accumulated spGFP-B in the core of the protein body. Asterisks in **(L)** indicate PB-II. Bars = 5 μm.

(O) Immunolabeling of an endosperm cell containing spGFP-B with anti-GFP antibody and a secondary antibody conjugated with 5-nm gold particles. Note that PB-I that contain spGFP-B are directly connected to the cisternal ER (ER). The arrow points to ribosomes bound to the membrane of the PB-ER complex. Bar = 200 nm.

targeting the fusion proteins to PB-I did not significantly alter the biogenesis of PB-I.

Because spGFP-AB, spGFP-B, and ABC-containing prolamins all contain CCxQL, it was hypothesized that disulfide bond formation at the dicysteine residues of CCxQL plays a role in the PB-I targeting of spGFP-AB and spGFP-B. As a result, the possible roles of the conserved amino acid residues Cys-78, Cys-79, and Leu-82 (in CCxQL) in the PB-I targeting of spG-GFP-AB were studied (Figure 4A). The *N*-glycosylation site attached to the N-terminal end of spGFP-AB (cf. Figures 3A and 4A) did not alter the efficiency of PB-I targeting (cf. Figures 4E and 3B). By contrast, spG-GFP-AB(C78S), in which Cys-78 was substituted with Ser (Figure 4B), was partitioned primarily into the lumen, rather than into PB-I, in dilated ER (Figures 4F and 4J). Interestingly, spG-GFP-AB(C79S), in which Cys-79 was substituted with Ser (Figure 4C), was targeted to PB-II (Figures 4G and 4K), although the efficiency of the PB-II targeting was much lower than that of spG-GFP-ABC (Figures 1C and 1D). Finally, substitution at Leu-82 with Phe [spG-GFP-AB(L82F), Figure 4D] reduced the PB-I targeting efficiency in dilated ER (Figures 4H and 4L). These results indicate that the intact CCxQL motif is necessary for efficient PB-I targeting of spG-GFP-AB.

When proteins were extracted from fine powders of seeds with SDS buffer under nonreducing conditions (see procedures in Methods), almost all of the processed glutelins and α-globulin were detected in the supernatant after centrifugation, whereas 13-kD prolamins and one-third of the proglutelins were detected in the pellet (Figure 5A). Interestingly, one-quarter of the spGFP was detected in the pellet (Figure 5B, lane 2), suggesting that GFP, which contains two Cys residues, formed intermolecular disulfide bonds with unidentified proteins. Half of the spG-GFP-ABC present was detected in the pellet (Figure 5B, lanes 3 and 4), suggesting that, like proglutelins, not all spG-GFP-ABC was transported to the PB-II matrix. By contrast, spG-GFP-ABC(C79F), spG-GFP-AB, and spG-GFP-AB(C78S) were detected almost exclusively in the pellet (Figure 5B, lanes 6, 8, and 10). A small but significant amount of spG-GFP-AB(C79S) was detected in the supernatant (Figure 5B, lane 11). It should be noted that significant amounts of BiP, PDI, and calnexin were detected in the pellet containing spG-GFP-AB(C78S) (Figure 5B, lane 10). Similarly, even larger amounts of BiP and PDI were detected in the pellet containing spG-GFP-ABC(C79F) (Figure 5B, lane 6).

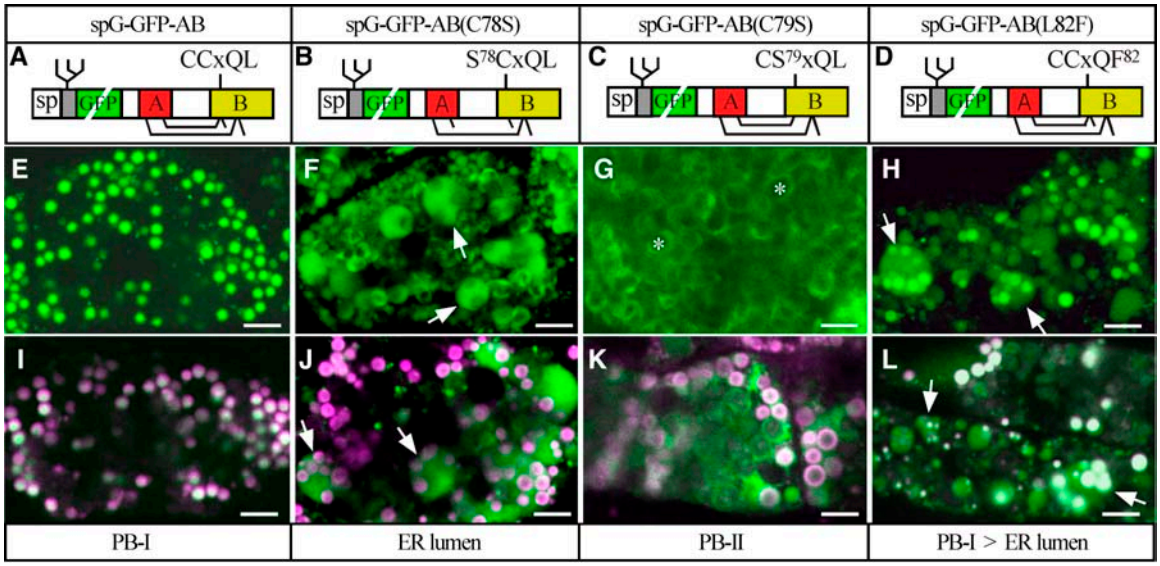

Figure 4. The CCxQL Motif Plays a Critical Role in Protein Sorting.

(A) to **(D)** Schemes of spG-GFP-AB **(A)** and mutated proteins containing C78S **(B)**, C79S **(C)**, and L82F **(D)** substitutions.
(E) and **(I)** Adding an *N*-glycosylation site to the PB-I–targeted spGFP-AB (Figure 3A) does not inhibit the PB-I targeting.
(F) and **(J)** The C78S substitution significantly reduces the efficiency of PB-I targeting. Note that spG-GFP-AB(C78S) is partitioned primarily into the lumen, rather than into PB-I, in the dilated ER indicated with arrows.
(G) and **(K)** spG-GFP-AB(C79S) is present mainly in the PB-II matrix.
(H) and **(L)** A small but significant amount of spG-GFP-AB(L82F) is present in the lumen of dilated ER (arrows), indicating that the L82F substitution reduced the efficiency of PB-I partitioning in dilated ER.
(E) to **(H)** Subaleurone cells at 12 DAA. The projections of seven GFP fluorescence images taken at 1-μm intervals along the *z* axis are shown. Bars = 5 μm.
(I) to **(L)** Subaleurone cells at 12 DAA. Fluorescent images of GFP and rhodamine B (PB-I protein bodies) in a single optical section are merged. Arrows indicate dilated ER. Asterisks indicate PB-II. Bars = 5 μm.

Prolamin Polymerization in Vitro

Rice λRM1, a 13-kD prolamin, contains four Cys residues, all of which are in the conserved motifs LxxC, CCxQL, and PxxC. Because little is known about which Cys residues in rice prolamins engage in intermolecular disulfide bonds, a series of experiments were conducted in vitro with λRM1 expressed in *Escherichia coli*. The protein was tagged with either the hemagglutinin (HA) or the myc epitope at the C-terminal end, producing RM1-HA and RM1-myc, respectively. Cys-135 (in PxxC) was substituted with Ala to produce RM1-HA(C135A) to evaluate whether Cys-135 engages in an intermolecular disulfide bond. The purified proteins tended to aggregate and randomly form disulfide bonds. However, certain conditions, such as low protein concentration, low temperature, and high concentrations of urea and reduced glutathione, proved to be effective in suppressing the aggregation of RM1-HA(C135A) (data not shown). Polymerization reactions were then conducted under conditions that allowed slow, but controlled, disulfide bond formation (but suppressed random oxidative reactions, which otherwise produced protein aggregates) (see procedures in Methods). If Cys-135 were involved in intermolecular disulfide bond formation, it was predicted that RM1-HA(C135A) would be unable to form oligomers. Based on this, it was believed that when RM1-myc and RM1-HA(C135A) were mixed in a ratio of 1:9, chances were high that RM1-myc, which contains Cys-135, would form an intermolecular disulfide bond with RM1-HA(C135A) rather than with another RM1-myc molecule. Figure 6 shows that a protein dimer that was detectable with an anti-myc antibody accumulated (lanes 5 to 8). By contrast, when RM1-myc was mixed with RM1-HA, which also contains Cys-135, in a ratio of 1:9, the dimer was short-lived and converted into larger oligomers, which were presumably too large to enter the polyacrylamide gel (Figure 6, lanes 1 to 4). Essentially identical results were obtained in protein gel blotting experiments with the antibody against the HA epitope (data not shown). These results indicate that Cys-135 indeed engaged in the polymerization of the epitope-tagged RM1 in vitro.

Characterization of the Vacuolar Targeting Signal in α-Globulin

The localizations of spGFP and spGFP-KDEL, which contains an ER retention signal (tetrapeptide KDEL) at the C terminus, were compared. Although spGFP was expected to be a secretory protein, its localization in the endosperm cells were essentially indistinguishable from those of spGFP-KDEL at all of the observed developmental stages. Both spGFP and spGFP-KDEL were contained in the ER (Figures 7C, 7F, and 8B). Note that

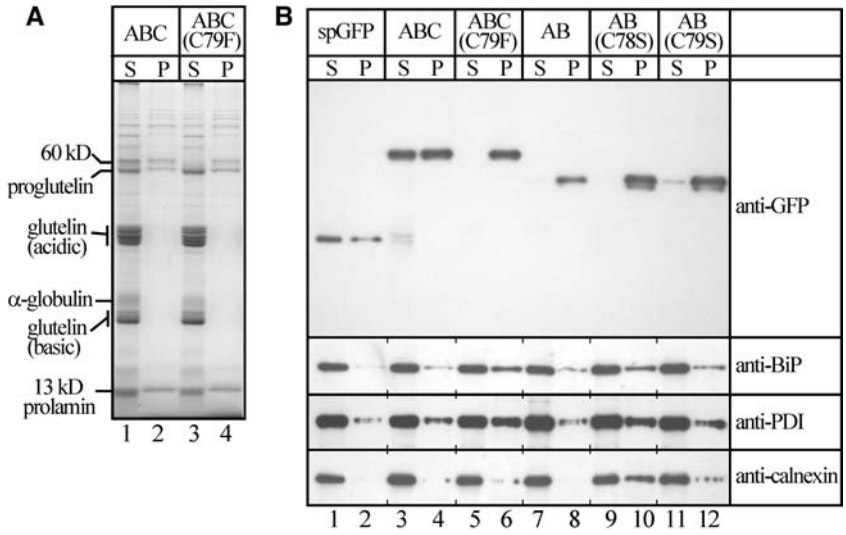

Figure 5. The Roles of ER Chaperons in Sorting Fusion Proteins.

(A) Proteins were extracted from mature seeds with SDS buffer, followed by centrifugation (see procedures in Methods). Proteins in the supernatants (S) and pellets (P) were separated on a 12% SDS-PAGE gel and stained with Coomassie Brilliant Blue. Lanes 1 and 2, spG-GFP-ABC (Figure 1A); lanes 3 and 4, spG-GFP-ABC(C79F) (Figure 1G). Note that almost all α-globulin and processed glutelins (acidic and basic subunits) were present in the supernatant, whereas significant amounts of proglutelins were present in the pellet fraction.

(B) Distinct extractabilities of fusion proteins and protein chaperons with the SDS buffer. The proteins in the supernatants (S) and pellets (P) were separated on a 12% SDS-PAGE gel, followed by protein gel blot analyses with antibodies against GFP, BiP, PDI, and calnexin. Lanes 1 and 2, spGFP (Figure 8A); lanes 3 and 4, spG-GFP-ABC; lanes 5 and 6, spG-GFP-ABC(C79F); lanes 7 and 8, spG-GFP-AB (Figure 4A); lanes 9 and 10, spG-GFP-AB(C78S) (Figure 4B); lanes 11 and 12, spG-GFP-AB(C79S) (Figure 4C).

dilated ER was found only in the early stages of seed development (cf. Figures 7C and 8B), and only after the amount of dilated ER diminished was spG-GFP-ABC observed in the matrix of PB-II (Figures 1C and 1D). These results indicate that the endomembrane system dramatically changed from the early stages (until ~10 DAA) to the middle stage (12 to 18 DAA) of seed development.

Transmission electron microscopy revealed that dilated ER was common at 10 DAA (Figures 7G and 7H). Interestingly, polysomes, some of which lined up in the shape of a disk (arrows in Figure 7G), were found on the membrane of the dilated part of the ER, indicating active translation at these sites. However, protein bodies in the lumen of dilated ER could not be detected. Different protocols for the preparation of the developing endosperm may be necessary to observe multiple PB-I in dilated ER by transmission electron microscopy.

Clear differences in protein localization between spGFP (Figures 7C and 8B) and spG-GFP-ABC (Figures 1B to 1D) suggest that a part of α-globulin facilitated the targeting of the fusion protein to PB-II. A peptide of this nature, if present, could be regarded as a vacuolar targeting signal (VTS). Because spG-GFP-AB(C79S) was also targeted to PB-II (Figures 4C, 4G, and 4K), it was predicted that a VTS might be present in either region A or B. When spA-GFP, which contains region A (Met-1 to Arg-59) (Figure 8C), was expressed in the endosperm, the protein was observed in the matrix of PB-II by 18 DAA (Figure 8D). Because the N-terminal end of mature α-globulin is Gln-23 (Komatsu et al., 1993), the VTS is presumably present in the peptide from Gln-23 to Arg-59, which includes the predicted helices H1 and H2 (Figure 1A). To determine whether H1 is sufficient as the VTS, the distribution of spΔA-GFP, in which Met-1 to Ser-43 was fused to GFP (Figure 8E), was analyzed. The localization of spΔA-GFP was indistinguishable from that of spA-GFP (Figure 8F), suggesting that the peptide from Gln-23 to

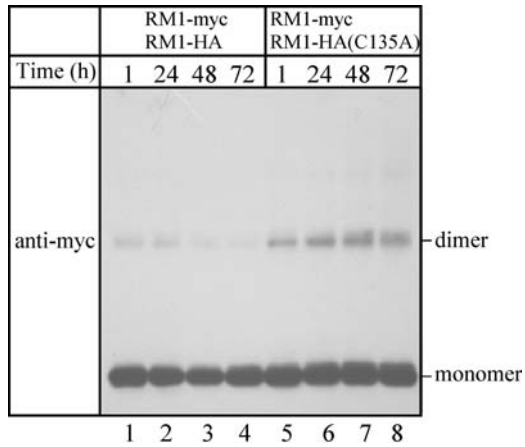

Figure 6. Prolamin Polymerization in Vitro.

Purified RM1-myc was mixed with either wild-type RM1-HA (lanes 1 to 4) or mutated RM1-HA(C135A) (lanes 5 to 8), and the polymerization reactions were allowed to continue for 1, 24, 48, or 72 h (see procedures in Methods). The proteins were separated on a 12% SDS-polyacrylamide gel under nonreducing conditions, followed by protein gel blot analysis with anti-myc antibody.

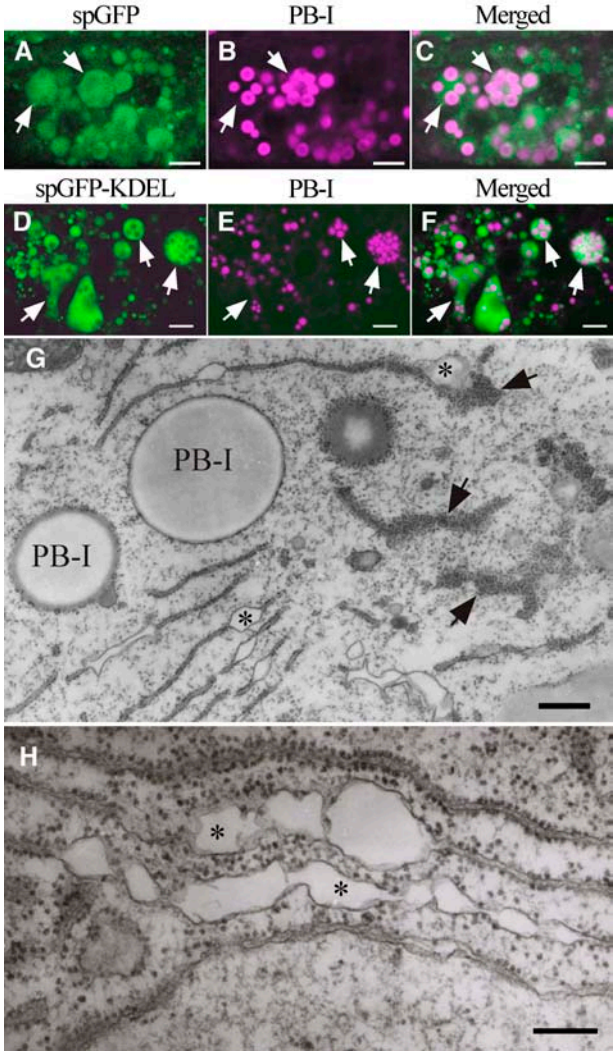

Figure 7. Dilated ER: A Prominent Organelle in the Early Stage of Endosperm Development.

(A) to **(C)** Distribution of spGFP **(A)** and PB-I **(B)** in a subaleurone cell at 10 DAA. The two images are merged in **(C)**. Note that many PB-I are present in dilated ER (arrows). Bars = 5 μm.
(D) to **(F)** Distribution of spGFP-KDEL **(D)** and PB-I **(E)** in a starchy endosperm cell at 7 DAA. The two images are merged in **(F)**. Arrows indicate dilated ER. Bars = 5 μm.
(G) Transmission electron micrograph of an endosperm cell (10 DAA) of a plant containing spGFP. Note that the dilated ER is covered with many polysomes (arrows). Asterisks indicate ER lumen. Bar = 500 nm.
(H) Enlarged view of dilated ER in the endosperm at 10 DAA. Asterisks indicate ER lumen. Bar = 200 nm.

Ser-43 was functionally sufficient as the VTS. The possibility of region C (Gln-148 to Tyr-186) containing another VTS was also investigated. The localization of spGFP-C, in which region C was fused at the C-terminal end of spGFP (Figure 8G), was similar to that of spGFP (Figure 8H), indicating that region C did not function as a VTS.

DISCUSSION

A Model for Prolamin Polymerization and the Evolution of Prolamin

The conserved motifs LxxC, CCxQL, and PxxC were identified in not only monomeric α-globulins and 2S albumins but also in polymeric prolamins, including rice λRM1, oat (*Avena sativa*) avenin-3, and wheat low molecular weight and HMW glutenins (Figure 9A). Figure 9B illustrates the relative locations of the four Cys residues (Cys-48, Cys-78, Cys-79, and Cys-171) in spG-GFP-ABC. Cys-48 (in LxxC) and Cys-78 (in CCxQL) form an intramolecular disulfide bond, which stabilizes the anti-parallel helices H2 and H3. Cys-79 (in CCxQL) and Cys-171 (in PxxC) form another intramolecular disulfide bond. The helical wheel

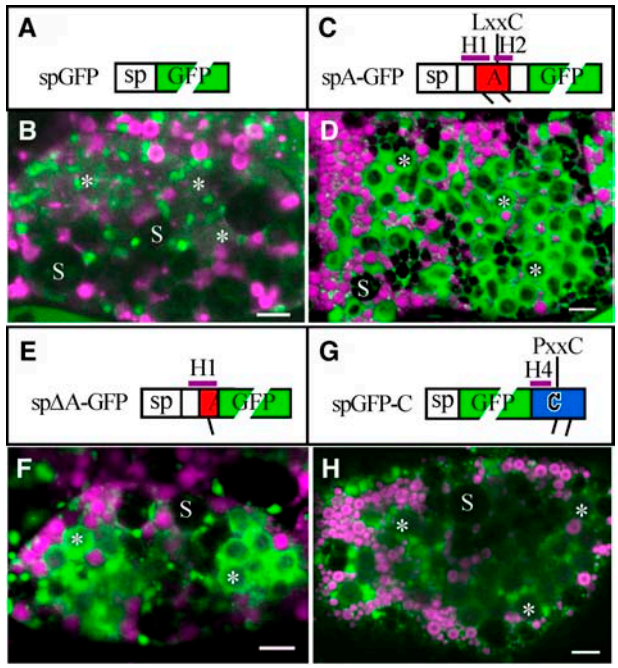

Figure 8. The A Region, Not the C Region, Targets GFP to PB-II.

(A) and **(B)** Scheme of spGFP **(A)** and the distributions of spGFP (green) and PB-I (magenta) in a subaleurone cell at 18 DAA **(B)**. Note that the prominent dilated ER containing multiple PB-I observed at 10 DAA (Figure 7C) is not recognizable.
(C) and **(D)** Scheme of spA-GFP **(C)**, which contains two unpaired Cys residues (Cys-36 and Cys-48, indicated with short lines) and two α-helices (H1 and H2) (see also Figure 1A), and distributions of spA-GFP (green) and PB-I (magenta) in a subaleurone cell at 18 DAA **(D)**.
(E) and **(F)** Scheme of spΔA-GFP **(E)**, which contains Cys-36 and the α-helix H1, and distributions of spΔA -GFP (green) and PB-I (magenta) in a subaleurone cell at 18 DAA **(F)**.
(G) and **(H)** Scheme of spGFP-C **(G)**, which contains two unpaired Cys residues (Cys-171 and Cys-178) and the α-helix H4, and distributions of spGFP-C (green) and PB-I (magenta) in a subaleurone cell at 18 DAA **(H)**. Note that both spA-GFP and spΔA-GFP are efficiently targeted to PB-II. By contrast, spGFP and spGFP-C are present mainly in the cisternal ER. Asterisks indicate PB-II. S, amyloplasts (which contain starch granules). Bars = 5 μm.

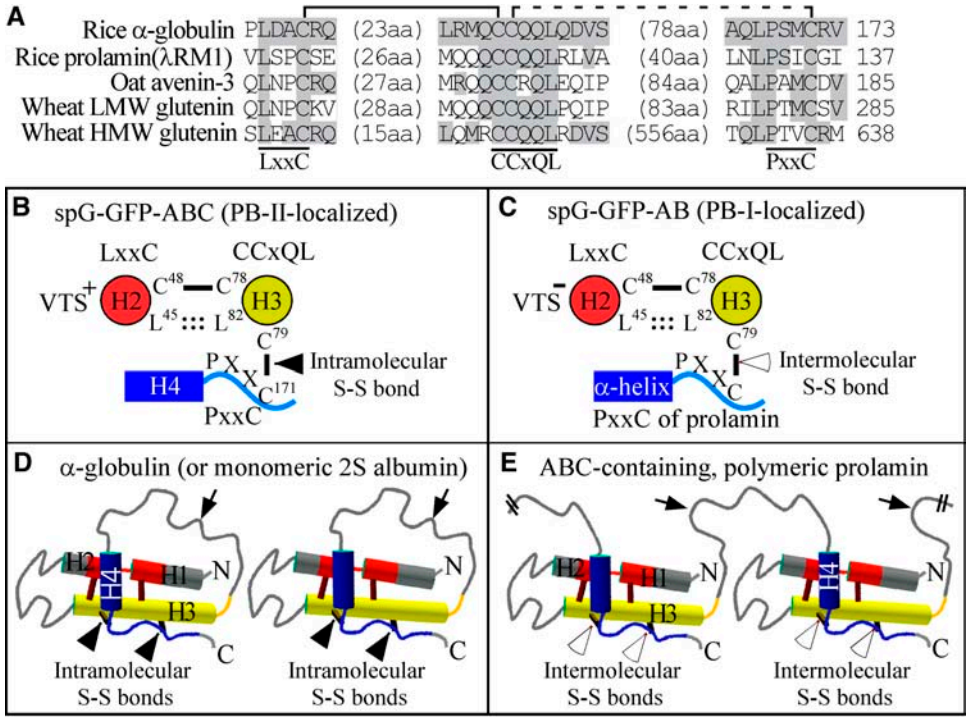

Figure 9. Molecular Evolution of Polymeric Prolamins from a Monomeric, ABC-Containing 2S Albumin.

(A) Both monomeric α-globulin and polymeric prolamins contain the LxxC, CCxQL, and PxxC motifs. The listed sequences are rice α-globulin (D50643), rice 13-kD prolamin λRM1 (BAA36697; see also Figure 6), oat avenin-3 (S48154), wheat low molecular weight glutenin (P10386), and wheat HMW glutenin 1Dy12 (X12929). All of the listed proteins except α-globulin are polymeric prolamins. Numbers in parentheses indicate the length of the amino acid (aa) residues between the presented sequences. Numbers at right indicate the positions of the last amino acid residues. Note that wheat HMW glutenin has an insertion of a large fragment (556 amino acids) between CCxQL and PxxC. The disulfide bond between LxxC and CCxQL (indicated with a solid line) is predicted to be intramolecular. The disulfide bond between CCxQL and PxxC (indicated with a dotted line) is intramolecular in monomeric α-globulin, although the corresponding disulfide bond in polymeric prolamins is predicted to be intermolecular.

(B) Helical wheel representation of H2 (Leu-45 to Gln-55) and H3 (Leu-74 to Glu-103) in spG-GFP-ABC (see also Figure 1A), presented as antiparallel helices. Note that the hydrophobic side chains of Leu-45 in LxxC, Leu-82 in CCxQL, and Pro-168 in PxxC could be buried in the core of the protein, which may facilitate the formation of disulfide bonds between Cys-48 and Cys-78 or Cys-79 and Cys-171. The VTS identified in region A (Gln-23 to Ser-43) is depicted as VTS^{+}.

(C) Helical wheel representation of H2 and H3 in spG-GFP-AB (see also Figure 4A). Cys-79 is predicted to form an intermolecular disulfide bond with the Cys residue in PxxC of the ABC-containing prolamin. This intermolecular disulfide bond formation is so efficient that the function of the peptide Gln-23 to Ser-43 as a VTS is suppressed (depicted as VTS^{-}).

(D) and **(E)** Schemes of α-globulin (or monomeric 2S albumin) and a possible mutation that could have played a role in the evolution of ABC-containing prolamins in cereals. In monomeric α-globulin or 2S albumin, regions A (red) and B (yellow) form antiparallel helices, which in turn interact with region C (blue) (intramolecular disulfide bonds are indicated with closed arrowheads). The helices H1, H2, H3, and H4 in α-globulin (see Figure 1A) roughly correspond to the helices Ia, Ib, II and III combined, and IV, respectively, in SFA-8 (Pantoja-Uceda et al., 2004). Accordingly, H3 may consist of two helices and a short loop between the two helices. It is predicted that a hypothetical mutation (indicated with arrows) in the so-called hypervariable loop between regions B and C (Pantoja-Uceda et al., 2004) changed the structure of the loop in such a way that the C region cannot interact with the antiparallel helices of the same molecule. Consequently, the C region of the mutated protein became free to interact with the antiparallel helices of another ABC-containing protein molecule and form intermolecular disulfide bonds (indicated with open arrowheads). N, N-terminal end; C, C-terminal end.

representation suggests that the hydrophobic side chains of Leu-45 (in LxxC) and Leu-82 (in CCxQL) may be buried in the core of the protein. Likewise, possible interactions between Pro-168 (in PxxC) and the antiparallel helices may facilitate the formation of the disulfide bond between Cys-79 and Cys-171. Indeed, the three-dimensional structure of SFA-8 indicates that the corresponding Leu residues in LxxC and CCxQL constitute the core of the protein close to the disulfide bonds (Pantoja-Uceda et al., 2004).

It was predicted that Cys-79 in spG-GFP-AB would form an intermolecular disulfide bond with the Cys residue in PxxC of endogenous prolamins (Figures 4A and 9C). It was demonstrated that Cys-135 in PxxC of λRM1 engaged in polymerization in vitro (Figure 6). In addition, substitutions at Cys-78, Cys-79, and Leu-82 in CCxQL demonstrated that all three of these residues were necessary for the efficient PB-I targeting of spG-GFP-AB (Figure 4). It is noted that significant amounts of PDI and BiP were detected in the pellet containing spG-GFP-ABC(C79F) or

spG-GFP-AB(C78S) (Figure 5B, lanes 6 and 10). These results suggest that the substitutions at Cys-78 or Cys-79 decreased the rates of PDI-catalyzed disulfide-interchange reactions or BiP-assisted protein-folding reactions, which probably led to the formation of insoluble protein complexes containing the ER chaperons and the fusion proteins. In this regard, studies of *esp2* rice mutants demonstrated that PDI is necessary for sorting prolamins and proglutelins in the ER lumen (Takemoto et al., 2002), suggesting that ABC-containing prolamins are substrates for PDI. Interestingly, the spG-GFP-AB(C78S) pellet also contained a significantly greater amount of calnexin (Figure 5B, lane 10). This result suggests that the lack of stable antiparallel helices in spG-GFP-AB(C78S) presumably induced prolonged interactions with the ER chaperons, including calnexin, which plays a role in the quality control of glycoproteins in the ER (Vitale, 2001).

Kreis et al. (1985) discussed the evolution of prolamin and 2S albumin (two major ABC-containing proteins) from a common ancestral gene. It is suggested here that the intermolecular disulfide bonds connecting polymeric prolamins were converted from intramolecular disulfide bond(s) that are indispensable in monomeric 2S albumins. Accordingly, a hypothetical mutation (indicated schematically with arrows in Figures 9D and 9E) in the so-called ''hypervariable loop'' between the B and C regions of a 2S albumin (Pantoja-Uceda et al., 2004) is proposed to have altered the loop structure in such a way that the 2S albumin was converted to a polymeric protein from which prolamins originated. Consistent with this theory, wheat HMW glutenin contains a large fragment insertion in the hypervariable loop (Figure 9A). Additional studies are necessary to evaluate whether and to what extent the predicted mode of disulfide bond formation exists in prolamin polymers in PB-I.

Disulfide Bond Formation Plays a Dominant Role in Protein Sorting in Rice Endosperm

Monitoring GFP fluorescence in transgenic rice by laser scanning confocal microscopy provided valuable insights into the protein-sorting mechanisms in the developing endosperm. Unusual dilated ER was often observed that contained multiple PB-I structures (Figures 1K, 3D, 4F, 4H, 4J, 4L, 7C, and 7F). Both spGFP and spGFP-KDEL were partitioned primarily into the lumen, rather than into PB-I, in dilated ER. These results suggest that the GFP itself does not have the structural characteristics that promote protein integration into PB-I in dilated ER and that the shape and size of PB-I are not necessarily determined by the enclosing ER membrane. Another unexpected result was that spGFP was not secreted to the apoplasm to detectable levels by laser scanning confocal microscopy (Figures 7C and 8B) or immunocytochemistry (data not shown). Rather, it was mainly contained in the cisternal ER. Torres et al. (2001) reported that a recombinant single-chain antibody with a KDEL tetrapeptide is localized in both PB-I and PB-II but not in the cell wall matrix in rice endosperm. Similarly, in transgenic wheat endosperm, phytase (secretory glycoprotein) accumulates in prolamin protein bodies but not in the apoplasm (Arcalis et al., 2004). All of these results indicate that when storage proteins accumulate on a large scale in the cereal endosperm, protein secretion from the Golgi to the apoplasm is not a major pathway in vesicle transport.

We demonstrated that the N-terminal peptide (Gln-23 to Ser-43) of α-globulin facilitated the PB-II targeting of GFP (spΔA-GFP, Figures 8E and 8F), which suggests that the peptide contains a VTS. The VTS may have interacted with an as-yet-unidentified membrane-bound receptor at the Golgi, which presumably promoted the transport of spΔA-GFP from the Golgi to PB-II. However, because spGFP was found mainly in the cisternal ER lumen (Figures 7C and 8B), a possible additional or alternative function of the peptide of Gln-23 to Ser-43 could be that it facilitated the ER exit of the protein (Barlowe, 2003) or prevented the retrograde transport of the protein from the *cis*-Golgi to the ER. Studies are under way to evaluate whether the peptide (Gln-23 to Ser-43) can also function as a VTS in other tissues.

Although spG-GFP-AB contains the VTS in Gln-23 to Ser-43, it accumulated very efficiently in PB-I (Figures 4A, 4E, and 4I). As discussed above, Figure 9C illustrates a possible molecular mechanism for the localization of spG-GFP-AB in PB-I: the efficient formation of an intermolecular disulfide bond between Cys-79 of spG-GFP-AB and the Cys residue in the PxxC motif of endogenous prolamin. Consistently, spG-GFP-AB(C79S) was targeted to PB-II (Figures 4C, 4G, and 4K). This event was interpreted to mean that the C79S substitution abolished the intermolecular disulfide bond with prolamin, which consequently restored the function of the VTS in Gln-23 to Ser-43. These results suggest that disulfide bond formation at the dicysteine residues of CCxQL played a dominant role in protein sorting in the ER lumen.

METHODS

Full-length cDNA clones for α-globulin (E11396), λRM1 (AU094552), BiP (AK065743 and AK066006), PDI (AK068268), and calnexin (AK069118) were obtained from the National Institute of Agrobiological Sciences (Tsukuba, Japan). The plasmid vectors pBlue-sGFP(S65T)-NOS KS and CaMV35S-sGFP(S65T)-Nos3′, both containing sGFP(S65T) (Niwa et al., 1999), were obtained from Y. Niwa (University of Shizuoka, Shizuoka, Japan). Rice (*Oryza sativa* cv Kitaake) and *Agrobacterium tumefaciens* EH105 were used for transformation. To attain anti-α-globulin antibody, a His-tagged polypeptide (Glu-26 to Tyr-186) was expressed in *Escherichia coli* and injected into rats. Similarly, antibodies to BiP, PDI, and calnexin were developed in rabbits by injecting the purified proteins from *E. coli*. The antibody to GFP was purchased from Santa Cruz Biotechnology (Santa Cruz, CA). The antibody to glutelins was described previously (Takemoto et al., 2002). Concanavalin A conjugated with peroxidase and antibodies to myc epitope and HA epitope were purchased from Sigma-Aldrich (St. Louis, MO). Endo H was purchased from New England Biolabs (Beverly, MA).

Gene Construction and Rice Transformation

To add a signal peptide to sGFP(S65T), complementary oligonucleotides encoding the N-terminal fragment from Met-1 to Ser-21 of a soybean (*Glycine max*) 11S globulin ($A_{1a}B_{1b}$ glycinin, accession number M36686) were annealed. This sequence was then inserted at the appropriate sites in pBlue-sGFP(S65T)-NOS KS, generating sp-GFP. The whole coding

region of spGFP-KDEL was amplified by PCR. A synthetic peptide (GELVSNGTVT), which contains an *N*-glycosylation site (Batoko et al., 2000), was inserted between the signal peptide and GFP by PCR, generating spG-GFP. The sequences of α-globulin that were fused to sp-GFP or spG-GFP include the following: Gly-21 to Tyr-186 and the 3′ untranslated region (spGFP-ABC and spG-GFP-ABC), Gly-21 to Gln-111 (spGFP-AB and spG-GFP-AB), Arg-68 to Gln-111 (spGFP-B), and Gln-148 to Tyr-186 (spGFP-C), which were amplified by PCR with the EST clone (E11396) as the template. Similarly, Met-1 to Ser-27 (spGFP), Met-1 to Arg-59 (spA-GFP), and Met-1 to Ser-43 (spΔA-GFP) were fused to the N-terminal end of sGFP(S65T). Amino acid substitutions in spG-GFP-AB(C78S), spG-GFP-AB(C79S), spG-GFP-AB(L82F), and spG-GFP-ABC(C79F) were introduced by PCR with mutagenic primers. The GFP fusion constructs were transferred into a binary vector derived from p8C-Hm (Onodera et al., 2001) containing the α-*globulin* promoter described previously (Wu et al., 1998) and the hygromycin phosphotransferase gene. Rice transformation was conducted as described previously (Goto et al., 1999).

Microscopy

Rice panicles were tagged when flowered and the seeds were harvested from 6 to 35 DAA. Developing seeds without the husk were embedded in 5% agarose and cross-sectioned through the middle portion of the seed in 100-μm-thick sections with a microslicer DTK-1000 (Dosaka EM, Kyoto, Japan). The sections were incubated in 1× PBS containing 1 nM rhodamine B for 30 min at room temperature, followed by washing twice with 1× PBS for 10 min. The samples were examined with a laser scanning confocal microscope (MicroRadiance2000; Bio-Rad, Richmond, CA) and its software (LaserSharp2000; Bio-Rad). Either cells adjacent to the aleurone cells, which are often called subaleurone cells, or the starchy endosperm cells that are one or two cell layers inward from the subaleurone cells were analyzed. Immunocytochemical analyses were performed as described previously (Takemoto et al., 2002). Red fluorescent images were converted to magenta with Adobe Photoshop (San Jose, CA). Section preparations of seeds at 10 DAA for transmission electron microscopy were essentially the same as those for immunogold labeling except that the samples were embedded in Epon instead of LR White.

Protein Extraction and Protein Gel Blot Analysis

Seed proteins were extracted from a fine powder of mature seeds with the following buffers: urea/SDS buffer (10 mg of seed powder per 0.35 mL): 50 mM Tris-HCl, pH 6.8, 8 M urea, 4% (w/v) SDS, and 20% (v/v) glycerol with or without 5% (v/v) β-mercaptoethanol; SDS buffer (1 mL per seed): 40 mM Tris-HCl, pH 6.8, and 0.5% (w/v) SDS. The samples were vigorously mixed at 25°C for 3 h and then centrifuged at 13,000*g* for 10 min at 25°C. When the urea/SDS buffer was used, the supernatant was applied directly onto a SDS-polyacrylamide gel. When the SDS buffer was used, the supernatant was mixed with an equal volume of 2× the protein sample buffer consisting of 125 mM Tris-HCl, pH 6.8, 20% (v/v) glycerol, 4% (w/v) SDS, 10% (v/v) β-mercaptoethanol, and 0.01% (w/v) Bromophenol Blue (the samples were applied directly onto a SDS-polyacrylamide gel). The pellet was washed with the SDS buffer (1 mL) and centrifuged as before, and the insoluble proteins in the pellet were then extracted with 0.5 mL of the urea/SDS buffer with 5% (v/v) β-mercaptoethanol. After centrifugation (13,000*g*, 10 min, 25°C), the supernatant was diluted fourfold with the urea/SDS buffer with β-mercaptoethanol for a direct comparison of the proteins of interest segregated into the two fractions (supernatant and pellet) using protein gel blot analyses. Proteins were resolved by SDS-PAGE with 12 or 14% separating (acrylamide: bisacrylamide = 29:1) and 4% stacking gels. When proteins were extracted with the urea/SDS buffer without β-mercaptoethanol for SDS-PAGE, care was taken not to reduce the proteins during electrophoresis. The gels were either stained with Coomassie Brilliant Blue R 250 or blotted onto polyvinylidene difluoride membranes for protein gel blotting with antibodies and an ECL kit (Amersham Pharmacia Biotech, Piscataway, NJ). When the antibody against α-globulin was used, which preferentially recognized the reduced form of the protein, the gel was soaked in a protein-transfer buffer containing 2% (v/v) β-mercaptoethanol for 5 min after electrophoresis. The detection of glycoproteins with concanavalin A conjugated with peroxidase followed the protein gel blotting procedures described above. For deglycosylation analysis with Endo H, seed proteins were extracted with the urea/SDS buffer with β-mercaptoethanol and precipitated using a chloroform/methanol method. The proteins were then resuspended in a reaction buffer and incubated in the presence or absence of Endo H at 37°C for 2 h according to the protocol recommended by the manufacturer.

Prolamin Polymerization in Vitro

PCR was used to introduce the myc epitope (EQKLISEEDL) and the HA epitope (YPYDVPDYA) at the C-terminal end of λRM1: RM1-myc and RM1-HA. The PCR fragments encoding the epitope-tagged proteins (starting from Ala-19 of λRM1) were inserted into the *Nco*I and *Xho*I sites in pET-23d (Novagen, Madison, WI), which contains a start codon at the N-terminal end and a His tag at the C-terminal end. A point mutation (C135A) was introduced by a standard PCR procedure with a mutagenic primer and RM1-HA as the template. The plasmids containing RM1 constructs were transferred to BL21-CodonPlus(DE3)-RIL (Stratagene, La Jolla, CA), and the inclusion bodies containing the epitope-tagged proteins were induced according to the manufacturer's instructions. The inclusion bodies were suspended in a detergent buffer consisting of 20 mM Tris-HCl, pH 7.5, 2 mM EDTA, 0.2 M NaCl, 1% (w/v) deoxycholic acid, 1% (w/v) Nonidet P-40, and 10 mM β-mercaptoethanol and sonicated on ice, followed by centrifugation at 13,000*g* for 10 min at 4°C. The supernatant was discarded, and the pellet was washed two more times with the same detergent buffer and once with another detergent buffer consisting of 20 mM Tris-HCl, pH 7.5, 0.5% Triton X-100, and 1 mM β-mercaptoethanol. The epitope-tagged proteins were then solubilized into monomers in an 8 M urea buffer: 20 mM Tris-HCl, pH 7.8, 8 M urea, and 1% (v/v) β-mercaptoethanol (RM1 proteins accounted for >99% of the total protein). The protein concentrations of the samples were estimated by SDS-PAGE using lysozyme as a protein standard. The samples were diluted with the 8 M urea buffer to 0.8 mg/mL and stored at −20°C. The polymerization reaction was conducted as follows. First, RM1-myc was mixed with either RM1-HA or RM1-HA(C135A) in a ratio of 1:9. The protein mixtures were reduced again with β-mercaptoethanol (the final concentration of β-mercaptoethanol was 1% [v/v]). Next, to precipitate the proteins together, 4 volumes of ice-cold acetone was added and this mixture was incubated at −20°C for 3 h. The samples were then centrifuged at 18,000*g* for 15 min at 4°C. The supernatant was discarded, and the pellet was washed once with 80% (v/v) ice-cold acetone, centrifuged as before, and dried briefly. The proteins were then dissolved in a buffer consisting of 20 mM Tris-HCl, pH 7.8, 8 M urea, and 10 mM reduced glutathione by vigorously mixing at 4°C. Finally, the sample was diluted with an equal volume of buffer consisting of 20 mM Tris-HCl, pH 7.8, and 2 mM oxidized glutathione. The final reaction mixtures (containing ~3.2 μg of proteins in 20 μL per reaction) consisted of 20 mM Tris-HCl, pH 7.8, 4 M urea, 5 mM reduced glutathione, and 1 mM oxidized glutathione. The polymerization reactions were conducted at 4°C and terminated at 1, 24, 48, and 72 h by adding 20 μL of deionized water and 40 μL of the 2× protein sample buffer without β-mercaptoethanol. The samples were then stored at −20°C until protein gel blot analyses were conducted.

ACKNOWLEDGMENT

This work was supported in part by the Research and Development Program for New Bio-Industry Initiatives from the Bio-Oriented Technology Research Advancement Institution.

Received January 6, 2005; accepted February 14, 2005.

REFERENCES

Arcalis, E., Marcel, S., Altmann, F., Kolarich, D., Drakakaki, G., Fischer, R., Christou, P., and Stoger, E. (2004). Unexpected deposition patterns of recombinant proteins in post-endoplasmic reticulum compartments of wheat endosperm. Plant Physiol. **136,** 3457–3466.

Barlowe, C. (2003). Signals for COPII-dependent export from the ER: What's the ticket out? Trends Cell Biol. **13,** 295–300.

Batoko, H., Zheng, H.Q., Hawes, C., and Moore, I. (2000). A Rab1 GTPase is required for transport between the endoplasmic reticulum and Golgi apparatus and for normal Golgi movement in plants. Plant Cell **12,** 2201–2217.

Bechtel, D.B., and Juliano, B.O. (1980). Formation of protein bodies in the starchy endosperm of rice (*Oryza sativa* L.): A re-investigation. Ann. Bot. **45,** 503–509.

Choi, S.B., Wang, C.L., Muench, D.G., Ozawa, K., Franceschi, V.R., Wu, Y.J., and Okita, T.W. (2000). Messenger RNA targeting of rice seed storage proteins to specific ER subdomains. Nature **407,** 765–767.

Crofts, A.J., Washida, H., Okita, T.W., Ogawa, M., Kumamaru, T., and Satoh, H. (2004). Targeting of proteins to endoplasmic reticulum-derived compartments in plants: The importance of RNA localization. Plant Physiol. **136,** 3414–3419.

Goto, F., Yoshihara, T., Shigemoto, N., Toki, S., and Takaiwa, F. (1999). Iron fortification of rice seed by the soybean ferritin gene. Nat. Biotechnol. **17,** 282–286.

Halford, N.G., Forde, J., Anderson, O.D., Greene, F.C., and Shewry, P.R. (1987). The nucleotide and deduced amino acid sequences of an HMW glutenin subunit gene from chromosome 1B of bread wheat (*Triticum aestivum* L.) and comparison with those of genes from chromosomes 1A and 1D. Theor. Appl. Genet. **75,** 117–126.

Komatsu, S., Kajiwara, H., and Hirano, H. (1993). A rice protein library: A data-file of rice proteins separated by two-dimensional electrophoresis. Theor. Appl. Genet. **86,** 935–942.

Kreis, M., Forde, B.G., Rahman, S., Miflin, B.J., and Shewry, P.R. (1985). Molecular evolution of the seed storage proteins of barley, rye and wheat. J. Mol. Biol. **183,** 499–502.

Krishnan, H.B., and White, J.A. (1995). Morphometric analysis of rice seed protein bodies: Implication for a significant contribution of prolamine to the total protein content of rice endosperm. Plant Physiol. **109,** 1491–1495.

Krishnan, H.B., Franceschi, V.R., and Okita, T.W. (1986). Immunochemical studies on the role of the Golgi complex in protein-body formation in rice seeds. Planta **169,** 471–480.

Krishnan, H.B., White, J.A., and Pueppke, S.G. (1992). Characterization and localization of rice (*Oryza sativa* L.) seed globulins. Plant Sci. **81,** 1–11.

Li, X., Wu, Y., Zhang, D.Z., Gillikin, J.W., Boston, R.S., Franceschi, V.R., and Okita, T.W. (1993). Rice prolamine protein body biogenesis: A BiP-mediated process. Science **262,** 1054–1056.

Li, X.X., and Okita, T.W. (1993). Accumulation of prolamines and glutelins during rice seed development: A quantitative-evaluation. Plant Cell Physiol. **34,** 385–390.

Martinez, I.M., and Chrispeels, M.J. (2003). Genomic analysis of the unfolded protein response in Arabidopsis shows its connection to important cellular processes. Plant Cell **15,** 561–576.

Mitsukawa, N., Konishi, R., Kidzu, K., Ohtsuki, K., Masumura, T., and Tanaka, K. (1999). Amino acid sequencing and cDNA cloning of rice seed storage proteins, the 13kDa prolamins, extracted from type I protein bodies. Plant Biotechnol. **16,** 103–113.

Muench, D.G., Ogawa, M., and Okita, T.W. (1999). The prolamins of rice. In Seed Proteins, P.R. Shewry and R. Casey, eds (Dordrecht, The Netherlands: Kluwer Academic Publishers), pp. 93–108.

Muench, D.G., Wu, Y., Zhang, Y., Li, X., Boston, R.S., and Okita, T.W. (1997). Molecular cloning, expression and subcellular localization of a BiP homolog from rice endosperm tissue. Plant Cell Physiol. **38,** 404–412.

Murzin, A.G., Brenner, S.E., Hubbard, T., and Chothia, C. (1995). SCOP: A structural classification of proteins database for the investigation of sequences and structures. J. Mol. Biol. **247,** 536–540.

Niwa, Y., Hirano, T., Yoshimoto, K., Shimizu, M., and Kobayashi, H. (1999). Non-invasive quantitative detection and applications of non-toxic, S65T-type green fluorescent protein in living plants. Plant J. **18,** 455–463.

Ogawa, M., Kumamaru, T., Satoh, H., Iwata, N., Omura, T., Kasai, Z., and Tanaka, K. (1987). Purification of protein body-I of rice seed and its polypeptide composition. Plant Cell Physiol. **28,** 1517–1527.

Onodera, Y., Suzuki, A., Wu, C.Y., Washida, H., and Takaiwa, F. (2001). A rice functional transcriptional activator, RISBZ1, responsible for endosperm-specific expression of storage protein genes through GCN4 motif. J. Biol. Chem. **276,** 14139–14152.

Oparka, K.J., and Harris, N. (1982). Rice protein-body formation: all types are initiated by dilation of the endoplasmic reticulum. Planta **154,** 184–188.

Pan, S.-J., and Reeck, G.R. (1988). Isolation and characterization of rice alpha-globulin. Cereal Chem. **65,** 316–319.

Pandya, M.J., Sessions, R.B., Williams, P.B., Dempsey, C.E., Tatham, A.S., Shewry, P.R., and Clarke, A.R. (2000). Structural characterization of a methionine-rich, emulsifying protein from sunflower seed. Proteins **38,** 341–349.

Pantoja-Uceda, D., Bruix, M., Gimenez-Gallego, G., Rico, M., and Santoro, J. (2003). Solution structure of RicC3, a 2S albumin storage protein from *Ricinus communis*. Biochemistry **42,** 13839–13847.

Pantoja-Uceda, D., Shewry, P.R., Bruix, M., Tatham, A.S., Santoro, J., and Rico, M. (2004). Solution structure of a methionine-rich 2S albumin from sunflower seeds: Relationship to its allergenic and emulsifying properties. Biochemistry **43,** 6976–6986.

Rost, B., and Sander, C. (1993). Prediction of protein secondary structure at better than 70% accuracy. J. Mol. Biol. **20,** 584–599.

Shewry, P.R., and Casey, R. (1999). Seed proteins. In Seed Proteins, P.R. Shewry and R. Casey, eds (Dordrecht, The Netherlands: Kluwer Academic Publishers), pp. 1-10.

Shewry, P.R., and Tatham, A.S. (1999). The characteristics, structures and evolutionary relationships of prolamins. In Seed Proteins, P.R. Shewry and R. Casey, eds (Dordrecht, The Netherlands: Kluwer Academic Publishers), pp. 11–33.

Shorrosh, B.S., Wen, L., Zen, K.C., Huang, J.K., Pan, J.S., Hermodson, M.A., Tanaka, K., Muthukrishnan, S., and Reeck, G.R. (1992). A novel cereal storage protein: Molecular genetics of the 19 kDa globulin of rice. Plant Mol. Biol. **18,** 151–154.

Takemoto, Y., Coughlan, S.J., Okita, T.W., Satoh, H., Ogawa, M., and Kumamaru, T. (2002). The rice mutant esp2 greatly accumulates the glutelin precursor and deletes the protein disulfide isomerase. Plant Physiol. **128,** 1212–1222.

Torres, E., Gonzalez-Melendi, P., Stoger, E., Shaw, P., Twyman, R.M., Nicholson, L., Vaquero, C., Fischer, R., Christou, P., and Perrin, Y. (2001). Native and artificial reticuloplasmins co-accumulate in distinct domains of the endoplasmic reticulum and in post-endoplasmic reticulum compartments. Plant Physiol. **127,** 1212–1223.

Vitale, A. (2001). Uncovering secretory secrets: Inhibition of endoplasmic reticulum (ER) glucosidases suggests a critical role for ER quality control in plant growth and development. Plant Cell **13,** 1260–1262.

Woo, Y.M., Hu, D.W.N., Larkins, B.A., and Jung, R. (2001). Genomics analysis of genes expressed in maize endosperm identifies novel seed proteins and clarifies patterns of zein gene expression. Plant Cell **13,** 2297–2317.

Wu, C.Y., Adachi, T., Hatano, T., Washida, H., Suzuki, A., and Takaiwa, F. (1998). Promoters of rice seed storage protein genes direct endosperm-specific gene expression in transgenic rice. Plant Cell Physiol. **39,** 885–889.

Yamagata, H., and Tanaka, K. (1986). The site of synthesis and accumulation of rice storage proteins. Plant Cell Physiol. **27,** 135–145.